

Finite-temperature Kondo effect in a realistic 5-fold-degenerate double quantum-dot device

Yaakov Kleeorin¹ and Yigal Meir^{1,2}

¹*Department of Physics, Ben-Gurion University of the Negev, Beer Sheva 84105, Israel*

²*The Ilse Katz Institute for Nanoscale Science and Technology,
Ben-Gurion University of the Negev, Beer Sheva 84105, Israel*

(Dated: December 14, 2024)

A novel highly correlated state is shown to emerge in a double-quantum-dot device, coupled in parallel to two leads, when the energy difference between the dots exactly compensates the difference between the intra- and inter-dot Coulomb interaction. Due to the five-fold degenerate low-energy space, the ground state is driven towards a special point between the Kondo and the mixed-valence regimes, where the transmission coefficient exhibits a sharp dip at the chemical potential, leading to a non-monotonic dependence of the conductance on temperature or voltage bias and the reemergence of the Kondo effect at finite temperatures. As that energy difference is easily controlled by gate voltage, our results are directly relevant to existing experimental setups.

PACS numbers:

Introduction. Ever since it has been realized [1–3] that a quantum dot (QD) can be used to probe the equilibrium and non-equilibrium properties of Kondo impurities, there has been a quest to find controllable experimental realizations of exotic Kondo states in quantum-dot devices. Indeed, there have been reports, for example, of experimental observations of the two-impurity Kondo effect [4], of the two-channel Kondo effect [5] and the $SU(4)$ Kondo effect [6–11] in QD systems.

Finding experimental realizations of the Kondo effect in highly degenerate systems is hindered by the fact that in a single dot, while higher degeneracy may arise from additional symmetries (such as in carbon nanotube dots), one cannot control the electron levels independently, while in double dots, where one can independently tune the energy levels in the separate dots, the intra-dot and inter-dot Coulomb interactions are usually significantly different, lifting the degeneracy. In this paper we study a specific method to increase the degeneracy in a double-dot system - by gate-tuning the energy difference between the two dots to compensate the difference in these Coulomb energies, one ends up with a five-fold degenerate two-electron system. As we will show below, based on both numerical-renormalization-group (NRG) and slave-boson mean field (SBMF) methods the conductance at that particular value of the parameters exhibits a very peculiar behavior - it is zero at zero temperature, but develops a narrow Kondo peak at higher temperature, only to decrease again at temperatures above the Kondo temperature. We will discuss in detail the physics behind these observations, which can be easily checked experimentally. In the following we will describe the model, the NRG and SBMF methods we have employed in exploring the model, and finally the results.

Model. The Hamiltonian that describes the two-QD

system, depicted in the inset to Fig.1, is given by

$$H_{2QD} = \sum_{m\sigma} \epsilon_m \hat{n}_{m\sigma} + \sum_m U_m \hat{n}_{m\uparrow} \hat{n}_{m\downarrow} + U_{12} \hat{n}_1 \hat{n}_2 \quad (1)$$

where $m = 1, 2$ denotes the QD index, $\hat{n}_{m\sigma} = d_{m\sigma}^\dagger d_{m\sigma}$,

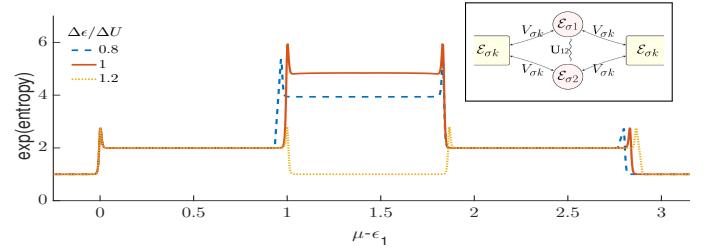


FIG. 1: Numerical-renormalization-group results for the (exponent of) the entropy in the double-dot system, as a function of chemical potential μ , for three values of the energy difference $\Delta\epsilon$ between the two dots, with $T = 0.33$, $\Gamma = 0.0001$. When $\Delta\epsilon$ is equal to the difference between the intra-dot (U) and inter-dot U_{12} Coulomb repulsion, there is a range of chemical potentials where the ground state develops a five-fold degeneracy. The sudden jumps in entropy indicate ground state crossing. Inset: The setup studied in this paper.

$\hat{n}_m = \sum_{\sigma} \hat{n}_{m\sigma}$ ($d_{m\sigma}^\dagger$ creates an electron on QD m with spin σ), and spin-degeneracy has been assumed (i.e. no magnetic field). In order to reduce the number of parameters, we will assume the same intra-dot interaction on both dots, $U_1 = U_2 = U$, though this assumption is not necessary, and our results will also hold when these energies are different. Without any loss of generalization, we assume $\epsilon_1 \leq \epsilon_2$. We will also assume that $U_{12} < U$, as one would expect experimentally. Under these assumptions, the six two-electron states have 3 distinct energies: the 4 states $|\sigma, \sigma'\rangle$, where each dot is occupied by a single electron (of spins σ and σ' , respectively) are degenerate with energy $2\epsilon_1 + \Delta\epsilon + U_{12}$, where $\Delta\epsilon \equiv \epsilon_2 - \epsilon_1$, while the state $|\uparrow\downarrow, 0\rangle$ where the two electrons occupy the

dot with the lower energy state, has energy $2\epsilon_1 + U$. The state $|0, \uparrow \downarrow\rangle$ is always higher in energy since $\Delta\epsilon > 0$ and $\Delta U \equiv U - U_{12} > 0$. Thus, as one increases $\Delta\epsilon$ from zero, the degeneracy of the ground state changes from being 4 to 5, for $\Delta\epsilon = \Delta U$, and then to a non-degenerate ground state for larger $\Delta\epsilon$ (Fig. 1). It is the physics around this special point that we will concentrate upon in this paper.

The full Hamiltonian of the two-QD system, connected in parallel to a single channel in the leads, is then given by

$$H = H_{2QD} + \sum_{\sigma k \in L, R} \epsilon_k c_{\sigma k}^\dagger c_{\sigma k} + \sum_{m\sigma k \in L, R} (V_{mk} d_{m\sigma}^\dagger c_{\sigma k} + h.c.), \quad (2)$$

where $c_{\sigma k}^\dagger$ creates an electron with spin σ in the left (L) or right (R) lead in momentum state k . For simplicity, the tunneling amplitude is chosen to be momentum (and spin) independent, $V_{mk} = V$.

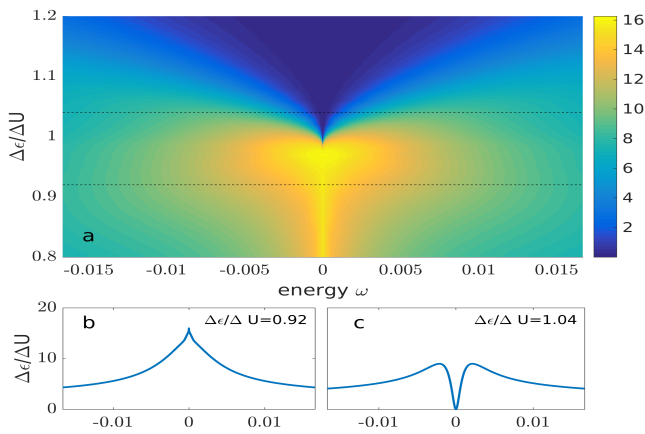


FIG. 2: (a) Numerical-renormalization-group results for the transmission spectral function, defined in the text, as a function of energy, and of $\Delta\epsilon$, at temperature $T = 0.03 \cdot 10^{-4}$. (b,c) Transmission spectral function for two values of $\Delta\epsilon$, denoted by the dotted line in (a). The Kondo peak for $\Delta\epsilon/\Delta U < 1$ develops a sharp dip in the vicinity $\Delta\epsilon \approx \Delta U$, before the Kondo peak disappears altogether for $\Delta\epsilon/\Delta U \gg 1$.

Numerical Renormalization Group Results. We first describe density-matrix numerical renormalization group (DM-NRG) results [23]. The expectation values and the transmission spectral function (see below), required for the evaluation of the conductance through the two-dot device [12], were calculated, assuming, for simplicity, equal couplings to the left and right leads, $\Gamma = \pi\rho V^2$, and equal and constant density of states ρ in the two leads, with a symmetric band of bandwidth D around the Fermi energy. In the following we set U to be the unit of energy. The bandwidth value in the calculations is $D = 3.33U$, the intra- and inter-dot interaction difference is $\Delta U = U/6$ and the coupling to the leads is $\Gamma = U/15$.

Defining the retarded Green functions $G_{ij,\sigma}^r(t-t') = -i\theta(t)\langle\{d_{i\sigma}(t), d_{j\sigma}(t')\}\rangle$ and the transmission spectral

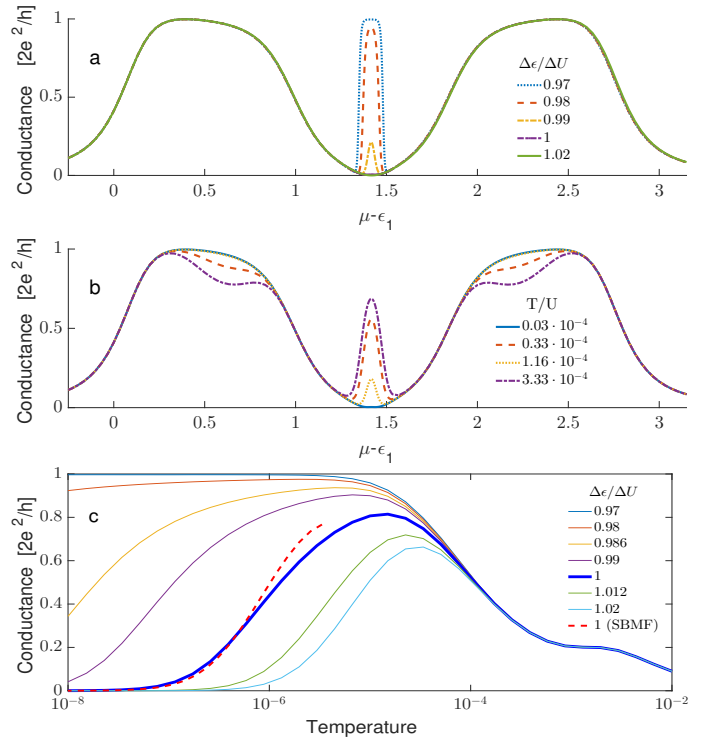


FIG. 3: Numerical-renormalization-group results for the conductance through the double-dot device as a function of chemical potential, for (a) various values of $\Delta\epsilon$, at $T = 0.03 \cdot 10^{-4}$ (all energies are in units of U , the intra-dot interaction), and (b) for various values of temperature, with fixed $\Delta\epsilon = \Delta U$. At zero temperature the conductance at the symmetry point $\mu = \mu_m$ is exactly zero, but a peak develops there at finite temperatures. (c) The temperature dependence of the mid-valley conductance, exhibiting a peak when $\Delta\epsilon \simeq \Delta U$.

function $t_\sigma(\omega; \mu, T) = \frac{1}{\pi} \text{Im}[\Gamma \sum_{ij} \tilde{G}_{ij,\sigma}^r(\omega)]$, where $\tilde{G}_{ij,\sigma}^r(\omega)$ is the Fourier transform of $G_{ij,\sigma}^r(t)$, the current is given by [12]

$$J = \frac{e}{h} \sum_{\sigma} \int t_\sigma(\omega; \mu, T) (f_L(\omega) - f_R(\omega)) d\omega \quad (3)$$

Fig. 2a depicts a two-dimensional plot of transmission spectral function as a function of energy ω and level-energy difference $\Delta\epsilon$, at the valley midpoint $\mu_m = \epsilon_1 + (U + 2U_{12} + \Delta\epsilon)/2$, for a fixed ΔU and low temperature $T = 0.03 \cdot 10^{-4}U$. For $\Delta\epsilon < \Delta U$ the transmission spectral function displays a sharp Kondo peak at the Fermi level (Fig. 2b) due to the fact that in this parameter regime each dot is singly occupied, giving rise to a finite magnetic moment which is screened at low temperatures here the two Kondo effects in the separate dots contribute constructively to the transmission). On the other hand, for $\Delta\epsilon > \Delta U$ the first dot is doubly occupied, while the second one is empty, and thus the only contribution to the spectral function at the center of the valley is from the tails of the standard Coulomb blockade peaks. Surprisingly, at the interface between these two regimes

the transmission spectral function develops a sharp dip in the middle of a wider peak, that reaches all the way to zero (Fig. 2c) (As we show below, this dip is caused by destructive interference between two mixed-valance Kondo contributions on opposite sides of the Kondo valley). This dip could easily be probed by transport measurements. In Fig. 3a we plot the conductance as a function of chemical potential, for different values of $\Delta\epsilon$ at the same temperature, $T = 0.03 \cdot 10^{-4}U$. Indeed, while for $\Delta\epsilon < \Delta U$ the conductance exhibits a sharp Kondo peak in the middle of the double-occupation valley [24], the conductance vanishes there around $\Delta\epsilon = \Delta U$, in accordance with the vanishing of the transmission spectral function at the chemical potential. Intriguingly, as shown in Fig. 3b, as temperature is increased, the mid-valley conductance for that value of $\Delta\epsilon$ increases, developing a sharp Kondo resonance, which is suppressed in yet higher temperatures. The dependence of the mid-valley conductance as a function of temperature, for various $\Delta\epsilon$, is plotted in Fig. 3c, where the maximum of conductance is clearly visible for $\Delta\epsilon \simeq \Delta U$. The emergence of a Kondo peak at finite temperatures at this value of the chemical potential, where the ground state is five-fold degenerate, is the central result of this paper, and will be explored in more detail in the following sections.

Slave-Boson Mean field Theory. In order to gain more insight into the physics behind the anomalous behavior around the special point discussed above, we have employed the slave-boson mean-field approach in the Kotliar-Ruckenstein formulation [13]. In order to accommodate the larger Hilbert space of the two-dot Hamiltonian, an enlarged boson space is introduced [14], where each boson accounts for one of the impurity dimer states: e for empty dimer, $p_{\sigma m}$ for single occupation of an electron with spin σ on dot m , x_m for two electrons on dot m , $y_{s\ell}$ for two electrons on different dots with total spin s and z-component of total spin ℓ , $h_{\sigma m}$ for triple occupation, with a missing electron on dot m with spin σ , and b for four electrons in the dimer. Since the system can be in only one of these states (or a linear combinations with total weight equal to unity), the bosons are constrained to have unit total occupation $I = e^\dagger e + \sum_{\sigma m} p_{\sigma m}^\dagger p_{\sigma m} + \sum_i x_i^\dagger x_i + \sum_{s\ell} y_{s\ell}^\dagger y_{s\ell} + \sum_{\sigma m} h_{\sigma m}^\dagger h_{\sigma m} + b^\dagger b$. Given the boson operators, the electron number operators are constrained to be $\hat{n}_{\sigma m} = \hat{Q}_{\sigma m}$, where $\hat{Q}_{\sigma m} = e^\dagger e + p_{\sigma m}^\dagger p_{\sigma m} + \sum_m x_m^\dagger x_m + y_{12\sigma}^\dagger y_{12\sigma} + \frac{1}{2} \sum_s y_{s0}^\dagger y_{s0} + h_{-\sigma m}^\dagger h_{-\sigma m} + \sum_\sigma h_{\sigma-m}^\dagger h_{\sigma-m} + b^\dagger b$. Including these constraints, the Hamiltonian (2) can be exactly mapped into the Slave Boson Hamiltonian, $H_{SB} =$

$H_{2QD} + H_{lead} + H_{cons}$, where:

$$H_{2QD} = \sum_{\sigma, m} \epsilon_m \hat{n}_{m\sigma} + U \sum_m x_m^\dagger x_m + U_{12} \sum_{sl} y_{sl}^\dagger y_{sl} + (U + 2U_{12}) \sum_{\sigma m} h_{\sigma m}^\dagger h_{\sigma m} + (2U + 4U_{12}) b^\dagger b \quad (4)$$

$$H_{cons} = \sum_{\sigma m} \lambda_{\sigma, m} (\hat{n}_{m\sigma} - \hat{Q}_{\sigma m}) + \lambda(I - 1)$$

$$H_{lead} = \sum_{\sigma k \in L, R} \epsilon_k c_{\sigma k}^\dagger c_{\sigma k} + \sum_{\sigma, m, k} z_{m\sigma} V_m c_{\sigma k}^\dagger d_{\sigma m} + h.c.$$

where $z_{m\sigma} = (1 - \hat{Q}_{\sigma, m})^{-1/2} (e^\dagger p_{\sigma m} + p_{-\sigma m}^\dagger x_m + p_{\sigma-m}^\dagger y_{12\sigma} + p_{-\sigma-m}^\dagger (y_{00} + y_{10})/2 + x_{-m}^\dagger h_{m-\sigma} + (y_{00}^\dagger + y_{10}^\dagger) h_{-\sigma-m}/2 + y_{12\sigma}^\dagger h_{\sigma-m} + h_{\sigma m}^\dagger b) (\hat{Q}_{\sigma, m})^{-1/2}$. In the mean-field approximation, all the boson operators are replaced by their expectation values, and one solves for these values using the self-consistent equations of motion and constraints (see Ref. [14] for further details). As a result of the mean-field approximation, one ends up with an effective non-interacting model, where the parameters of the two dots are renormalized ($\epsilon_m \rightarrow \tilde{\epsilon}_m \equiv \epsilon_m + \lambda_{\sigma m}$ and $V_m \rightarrow \tilde{V}_m \equiv z_{m\sigma} V_m$), where we assume spin degeneracy, so the bosonic expectation values are independent of σ .

Given the solution for the parameters $\tilde{\epsilon}_m$ and $\tilde{\Gamma}_m$ of the effective non-interacting model, the transmission spectral function is given by

$$t(\omega; \mu, T) \equiv \left| \frac{(\omega - \tilde{\epsilon}_1) \tilde{\Gamma}_2 + (\omega - \tilde{\epsilon}_2) \tilde{\Gamma}_1}{(\omega - \tilde{\epsilon}_1 + i \tilde{\Gamma}_1)(\omega - \tilde{\epsilon}_2 + i \tilde{\Gamma}_2) + \tilde{\Gamma}_1 \tilde{\Gamma}_2} \right|^2, \quad (5)$$

where $\tilde{\Gamma}_m = \pi \rho \tilde{V}_m^2$. The temperature and chemical potential dependence of $t(\omega; \mu, T)$ arise from the dependence of the renormalized parameters $\tilde{\epsilon}_m$ and $\tilde{\Gamma}_m$ on these parameters. The resulting conductance, as a function of chemical potential, for the special point $\Delta\epsilon = \Delta U$ is depicted in Fig. 4a. The results of the SBMF approximation closely resemble those of the accurate NRG calculation (except for an overestimated width of the middle region), with the conductance going to zero at the symmetry point, only to increase with increasing temperature, giving rise again to a finite-temperature Kondo effect. The temperature dependence of the conductance at $\Delta\epsilon = \Delta U$ in the SBMF treatment is plotted along with the NRG results in Fig. 3c. The similarity between NRG and SBMF results gives additional credence to this approximation, at least in this parameter regime [25]. In the following we will utilize the additional information, available within the SBMF approximation, to shed light on the physics behind the peculiar finite-temperature Kondo effect at the symmetry point.

Within the SBMF theory, the emergence of a Kondo peak in the spectral function, and the resulting peak in the conductance, are due to the renormalization of the effective energies $\tilde{\epsilon}_i$ toward the chemical potential. For a

single dot, in the Coulomb-blockade valley corresponding to total unit occupation, each spin state is half-occupied, on average. Thus, in order to obtain the same occupation by an effective non-interacting model, the energy of each spin state lies exactly at the Fermi energy, leading to a resonance at that energy which is interpreted as the Abrikosov-Suhl resonance associated with the Kondo effect (for a review, see [15]). On the other hand, in the single-dot Coulomb-blockade valleys which correspond to zero or double occupation, the renormalized energy levels are shifted to well above or below the Fermi level, leading to suppression of the spectral function at the Fermi energy. Thus, in order to understand the features in the spectral function in the double-dot system, one needs to determine corresponding energy shifts. For $\Delta\epsilon \gg \Delta U$, dot 1 is doubly occupied, while dot 2 is empty and so $\tilde{\epsilon}_1$ is shifted to well below the Fermi energy, while $\tilde{\epsilon}_2$ to well above it, explaining the absence of any feature in the spectral function near the Fermi energy in that regime. In the vicinity of $\Delta\epsilon = \Delta U$ and the five-fold degenerate point the average occupation of dot 1 drops to $n_1 = 6/5$ while that of dot 2 rises to $n_2 = 4/5$ [26]. Thus in that case, the energies $\tilde{\epsilon}_1$ and $\tilde{\epsilon}_2$ will straddle the Fermi energy symmetrically, while the factor $|\tilde{\epsilon}_i - \mu|/\tilde{\Gamma}$ remains finite, to allow for that fractional occupation. Thus in that specific value of $\Delta\epsilon$ the system is shifted into a particular point in the mixed-valence regime. Moreover, the two symmetric Abrikosov-Suhl resonances give rise to the exact same transmission amplitude, which interfere destructively due to a phase difference of π between sub-resonance and sup-resonance transmission through the individual dots. This interference is the origin of the central dip and the finite-temperature effect.

Experimental predictions. The predicted features in the conductance, either as a function of gate voltage (Fig. 3a and b) or as a function of temperature (Fig. 3c), can be easily checked in the double-dot setup, depicted in the inset of Fig. 1, where each dot is controlled by a different gate voltage. The intra- and inter-dot interactions, U and U_{12} , and consequently $\Delta U = U - U_{12}$, are usually determined by the geometry of the system and cannot be easily modified. However the energy difference between the two dots, $\Delta\epsilon = |\epsilon_1 - \epsilon_2|$, can be readily tuned by changing the relative voltage between the two gates controlling the separate dots. Thus, for a given setup, one can change this relative voltage until the Kondo peak at the valley midpoint is suppressed and the conductance vanishes. As discussed above, this should happen around the point where $\Delta\epsilon$ reaches the value ΔU . Note that as the value of $\Delta\epsilon$ decreases, one expects [16–18] sharp features in the conductance, associated with abrupt switching in level occupations [19, 20]. It would be interesting to explore the interplay of this physics with the one discussed in this paper.

In addition to the features in the linear-response conductance, the predicted dip in the spectral function

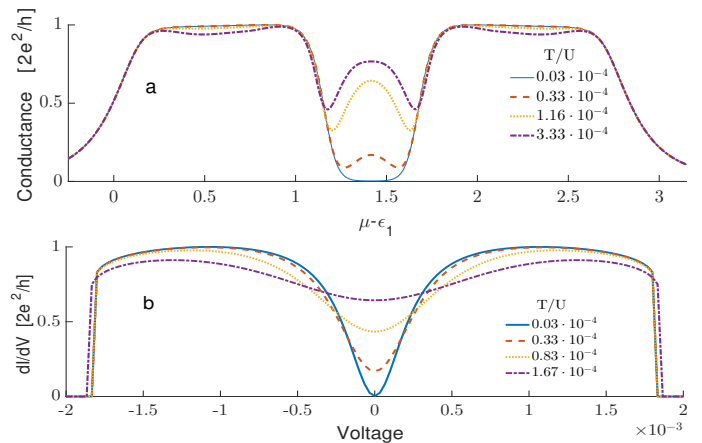


FIG. 4: Slave-boson mean-field results. (a) The linear-response conductance through the double-dot device as a function of chemical potential, for various values of temperature, with fixed $\Delta\epsilon = \Delta U$. Other parameters are the same as in Fig. 3b, except Γ which is smaller by a factor of 2 than the NRG calculation. (b) The differential conductance ($\frac{dI}{dV}$) at the mid point as a function of positive bias (symmetric to the negative values) $\Gamma = U/30$.

can be probed experimentally by measuring the voltage-dependent differential conductance $G(V)$ through the double-dot system for that value of $\Delta\epsilon$. Fig 4b depicts $G(V)$ for several temperatures, using the SBMF approximation. As one might expect, $G(V)$ exhibits a peak away from zero bias, corresponding to the shift of the peaks in the spectral function from the Fermi energy. At high enough voltage the Kondo effect is suppressed, though in the SBMF approach, this appears as an unphysical abrupt transition. We also expect signatures of the dip at the spectral function for other transport phenomena, such as the thermopower.

Notice that in the above we assumed that the two dots connect to the same channel in the leads, which led to the destructive interference and the dip at the fivefold-degenerate point discussed above. This corresponds to a situation where the electrons from each dot couple to the same electronic wavefunction in the leads. While this can be achieved through careful alignment of the dots, the usual experimental situation is that the electronic wavefunctions in the leads that couple to the separate dots are not identical, though they might have a significant overlap. Thus, in order to evaluate the conductance in this case one has to include contributions from a two-channel model, where each dot couples to a different state in the leads. While the separate spectral function of each dot will be identical in this case to the single-channel case, the conductance formula will be different, and in particular, here the contribution of the two channels to the conductance will be additive, instead of the destructive interference observed in the single-channel case. Consequently, we expect that the conductance will not strictly vanish in the middle of the valley, for $\Delta\epsilon = \Delta U$, but will have a finite minimal value that depends on geometrical

details.

Comparison to other models and conclusions. The results we have presented suggest that for a fixed ΔU , changing the parameter $\Delta\epsilon$ can tune the system away from the five-fold degenerate point towards the standard Kondo regime. For $\Delta\epsilon = \Delta U$ the conductance, as was shown in Fig. 3c, exhibits a peak with decreasing temperature, eventually going to zero at zero temperature. As $\Delta\epsilon$ decreases away from ΔU , the peak increases and shifts to lower temperature, until, at low enough values of $\Delta\epsilon$, one reproduces the standard Kondo effect, where the conductance monotonically increases towards $G = 2e^2/h$. These results are very similar to the case where $\Delta\epsilon, \Delta U = 0$, but with ferromagnetic coupling J between the two dots (Fig. 5). In this case, for an increasing J the Kondo effect is suppressed and one finds a similar behavior to the model discussed in this paper. Note, however, that in the case of an antiferromagnetic coupling between the dots (or tunneling between them), there are naturally two scales in the problem - the Kondo temperature T_K associated with each dot, and the magnetic coupling J between them - which are independent. The spectral function in this case will exhibit two peaks, each of width T_K , split by energy J . Thus this latter case leads to a two-stage Kondo process, where as one lowers the temperature, one observes a certain behavior when the temperature is below one scale and larger than the other, and a different behavior when the temperature is lower than both of them. As discussed above, for the case $\Delta\epsilon = \Delta U$ there is a single scale in the problem, as the width of the peaks in the spectral function, as observed both in the NRG and the SBMF calculations, is, up to a factor, the same as the splitting between them. Moreover, unlike the parameter $\Delta\epsilon$ that can be easily changed continuously, it is very difficult to tune experimentally a parameter like the magnetic interaction J . Nevertheless, the resemblance of our data to the antiferromagnetic double-dot case, where a quantum phase transition between the two phases may occur [21], raises the question whether there might be also a quantum phase transition in the current model. As the SBMF theory, which does give rise to an abrupt change in the saddle point solution as a function of $\Delta\epsilon$, is not reliable in differentiating between a smooth crossover and an abrupt phase transition, the current numerical-renormalization-group data are not accurate enough to answer this question with certainty. We hope to address this intriguing question in the future.

We thank P. Moca and G. Zarand for scientific discussions and help with the DM-NRG code. YM acknowledges support from ISF grant 292/15.

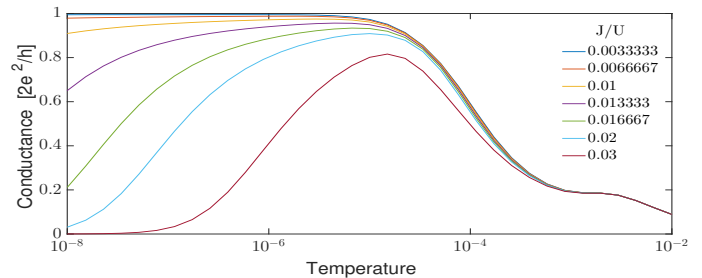


FIG. 5: Numerical-renormalization-group results for the conductance through a double-dot device with $\Delta\epsilon = 0, U_{12} = 0$, but with antiferromagnetic interaction J between the dots. Increasing J displays similar behavior to Fig. 3c.

- [1] L. I. Glazman and M. E. Raikh, *47*, 1773 (1988).
- [2] T. K. Ng and P. A. Lee, *Phys. Rev. Lett.* **61**, 1768 (1988).
- [3] Y. Meir, N. S. Wingreen, and P. A. Lee, *Phys. Rev. Lett.* **70**, 2601 (1993).
- [4] H. Jeong, A. M. Chang, and M. R. Melloch, *Science* **293**, 2221 (2001).
- [5] R. M. Potok, I. G. Rau, H. Shtrikman, Y. Oreg, and D. Goldhaber-Gordon, *Nature* **446**, 167 (2007).
- [6] P. Jarillo-Herrero, J. Kong, H. S. J. van der Zant, C. Dekker, L. P. Kouwenhoven, and S. De Franceschi, *Phys. Rev. Lett.* **94**, 156802 (2005).
- [7] A. Makarovski, A. Zhukov, J. Liu, and G. Finkelstein, *Phys. Rev. B* **75**, 241407 (2007).
- [8] F. B. Anders, D. E. Logan, M. R. Galpin, and G. Finkelstein, *Phys. Rev. Lett.* **100**, 086809 (2008).
- [9] G. C. Tettamanzi, J. Verduijn, G. P. Lansbergen, M. Blaauboer, M. J. Caldern, R. Aguado, and S. Rogge, *Phys. Rev. Lett.* **108**, 046803 (2012).
- [10] A. Hubel, K. Held, J. Weis, and K. v. Klitzing, *Phys. Rev. Lett.* **101**, 186804 (2008).
- [11] A. J. Keller, S. Amasha, I. Weymann, C. P. Moca, I. G. Rau, J. A. Katine, H. Shtrikman, G. Zarnd, and D. Goldhaber-Gordon, *Nat Phys* **10**, 145 (2014).
- [12] Y. Meir and N. S. Wingreen, *Phys. Rev. Lett.* **68**, 2512 (1992).
- [13] G. Kotliar and A. Kapitulnik, *Phys. Rev. B* **33**, 3146 (1986).
- [14] H. Oguchi and N. Taniguchi, *J. Phys. Soc. Jpn.* **79**, 054706 (2010).
- [15] A. C. Hewson, *The Kondo Problem to Heavy Fermions* (Cambridge University Press, 1997).
- [16] C. A. Busser, E. Vernek, P. Orellana, G. A. Lara, E. H. Kim, A. E. Feiguin, E. V. Anda, and G. B. Martins, *Phys. Rev. B* **83**, 125404 (2011).
- [17] I. L. Ferreira, P. A. Orellana, G. B. Martins, F. M. Souza, and E. Vernek, *Phys. Rev. B* **84**, 205320 (2011).
- [18] Y. Kleeorin and Y. Meir, *Phys. Rev. B* **96**, 045118 (2017).
- [19] R. Baltin, Y. Gefen, G. Hackenbroich, and H. A. Weidenmüller, *Eur. Phys. J. B* **10**, 119 (1999).
- [20] P. G. Silvestrov and Y. Imry, *Phys. Rev. Lett.* **85**, 2565 (2000).
- [21] B. A. Jones, C. M. Varma, and J. W. Wilkins, *Phys. Rev. Lett.* **61**, 125 (1988).
- [22] W. Izumida, O. Sakai, and S. Tarucha, *Phys. Rev. Lett.* **87**, 216803 (2001).
- [23] We used the open-access Budapest Flexible DM-NRG code, <http://www.phy.bme.hu/dmnrng/>; O. Legeza, C. P. Moca, A. I. Toth, I. Weymann, G. Zarand,

arXiv:0809.3143 (2008) (unpublished)

- [24] a conductance peak at the mid-valley, similar in appearance to our case, also appears near the singlet-triplet transition, tuned by a magnetic field as studied in [22]
- [25] The above comparison was done for $\Gamma_{NRG} = 2\Gamma_{SBMF}$, which is a known discrepancy between NRG and SBMF [14].
- [26] In fact, in the NRG calculation, due to the effective shifts in the dot energies due to the coupling to the leads, the occupations at the point $\Delta\epsilon = \Delta U$ deviate from these values.